Poly(ethylene-*co*-vinyl acetate)/Calcium Phosphate Nanocomposites: Mechanical, Gas Permeability, and Molecular Transport Properties

P. Selvin Thomas,[1,2] P. A. Sreekumar,[1,2] Abi Santhosh Aprem,[3] Sabu Thomas[1]

[1]*Department of Chemical Engineering, King Fahd University of Petroleum and Minerals, Dhahran, Saudi Arabia 31261*
[2]*School of Chemical Sciences, Mahatma Gandhi University, Kottayam, Kerala, India 686560*
[3]*Corporate R&D Center, HLL Lifecare Limited, Trivandrum, Kerala, India 695012*

Received 12 October 2010; accepted 21 August 2010
DOI 10.1002/app.33238
Published online 8 December 2010 in Wiley Online Library (wileyonlinelibrary.com).

ABSTRACT: Poly(ethylene-*co*-vinyl acetate) (EVA)-based nanocomposites were prepared by melt mixing in an internal mixer with nanocalcium phosphate in different weight percentages. The nanocalcium phosphate with 10-nm size was prepared by the polymer-induced crystallization technique. The mechanical properties as well as the gas permeability tests were performed to analyze the effect of nanofiller incorporation in to the polymer. Molecular transport of different solvents such as water, benzene, and *n*-heptane was undertaken at room temperature for EVA nanocomposites with 0, 3, and 5% filler loading. Among the three, water showed less uptake and benzene showed maximum uptake. Transport parameters such as diffusion coefficient, sorption coefficient, and permeation coefficient were calculated, and all of them showed a decrease with respect to the filler loading. First-order kinetics model was applied to investigate the transport kinetics. Also, the sorption curves were compared to theoretical predictions and found to be in good agreement except for water. © 2010 Wiley Periodicals, Inc. J Appl Polym Sci 120: 1974–1983, 2011

Key words: poly(ethylene-*co*-vinyl) acetate; calcium phosphate; nanocomposites; gas permeability; molecular transport

INTRODUCTION

Polymer nanocomposites are a special class of polymer materials with ultrafine phase dispersion of the order of a few nanometers that show very interesting properties often very different from those of conventional filled polymers.[1–4] The presence of these nanoparticles mostly improve the elastic modulus without decreasing the elongation at break and do not decrease the rheological and processing behavior and the optical properties of the polymer matrix. All these properties have been measured considering a possible use of these new materials for different applications. The number of particles dispersed in nanocomposites is very high compared to microcomposites due to the difference in size of the particles or fillers.

The diffusion and transport characteristics of solvents through filled polymers depend upon the nature of the fillers, the degree of adhesion, and their compatibility with the polymer matrix. If the filler used is inert and if it is compatible with the polymer matrix, it will take up the free volume within the polymer matrix and create a tortuous path for the permeating molecules. The degree of tortuosity is dependent on the volume fraction and the shape and orientation of the particles. On the other hand, if the filler is incompatible with the polymer matrix, voids tend to occur at the interface, which tends to increase the free volume of the system and thereby increases the permeability through it.[5] This difference is important in determining the properties of the resultant composites including mechanical, thermal, and barrier properties.

Transport properties of polymers are strongly dependent on the crosslinking, the nature of additives, and penetrant size. The transport properties of various rubber/rubber, thermoplastic elastomers, interpenetrating networks, and natural fiber, and particulate filled blends and composites have been studied.[6–12] The diffusion process is a kinetic parameter depending on the free volume within the material, segmental mobility of polymer chains, and the size of the penetrant molecule.[13] The study of diffusion in polymers deserves from two points of view: first, as a phenomenon that results in ageing, and second, as a tool that allows us to investigate the structure and composition of a material.[13]

Stephen et al.[14] studied the transport properties of nanostructured layered silicates reinforced natural

Correspondence to: S. Thomas (sabuchathukulam@yahoo.co.uk or selvin@kfupm.edu.sa).

rubber; carboxylated styrene butadiene rubber and their 70/30 blends using solvents, such as benzene, toluene, and *p*-xylene. The nanocomposites exhibited reduced absorption rate. This is because of increased polymer/filler interaction, which resulted in tortuosity of path and the reduced transport area in polymeric composites. It was found that the diffusion coefficient of filled samples decreased as a function of concentration of silicates. Solvent resistance of the samples increased upon the addition of nanostructured silicates due to the intercalation of rubber chain into the layers. It will result in nanometric level of dispersion of silicates into the polymer matrix. It was observed that, as the size of the permeant molecule increased, the solvent uptake of polymer decreased in the order of benzene > toluene > *p*-xylene. Samples showed an anomalous diffusion behavior rather than Fickian. The same authors investigated transport properties of microcomposites of natural rubber; carboxylated styrene butadiene rubber and their 70/30 blend using solvents, such as benzene, toluene, and *p*-xylene.[15] Here, also a reduction in sorption occurred due to the tortuous pathway created in the system.

Ethylene vinyl acetate is a copolymer, which has many industrial and pharmaceutical applications. Ethylene vinyl acetate-based nanocomposites have attracted great deal of attention as a simple and cost effective method of enhancing polymer properties by the addition of a small amount of properly designed filler, leading to the creation of composite materials where the reinforcing particles can be distributed in the polymeric matrix at the nanometer level.[16–20] There were reports on the effective use of various nanofillers on the mechanical, thermal, rheological, and flame-retardant aspects of EVA nanocomposites very recently. Nanocalcium phosphate particles were prepared by the polymer-mediated synthesis technique as reported earlier.[21–26] The nanoparticles used for this study were characterized by different analytical techniques, and the size was around 10 nm. These nanopaticles has high degree of protein carrying capacity and have a stable shape over a period of time. In addition to the small size, phosphates are reported to impart very good mechanical strength, flame retardancy, and barrier properties to the polymer matrix.[27–30]

The incorporation of these calcium phosphate nanoparticles into the EVA matrix and the characterization and analysis of the composites is highly useful to elucidate the effect of nanofiller on the mechanical as well as barrier properties. To the best of our knowledge, there were no reports on the effect of nanocalcium phosphate on EVA with respect to the mechanical and barrier properties. Therefore, we analyzed the nanocomposites of EVA with nanocalcium phosphate in various filler content in terms of mechanical behavior gas permeability and transport properties.

TABLE I
Characteristics of EVA

Characteristics	
Vinyl acetate (%)	18.00
Melt flow index (kg/600 s) (ASTM D 1238)	2.00×10^{-3}
Intrinsic viscosity ($m^3\ kg^{-1}$) (ASTM D 2857)	0.017
Density (kg/m^3) (ASTM D 1505)	0.94×10^{-3}
Vicat softening point (°C) (ASTM D 1525)	59.0
T_g (°C) (ASTM D 3417)	−10

MATERIALS AND METHODS

Materials

Poly(ethylene-*co*-vinyl acetate)

Poly(ethylene-*co*-vinyl acetate) (EVA) with 18% vinyl acetate content (Pilene-1802) was procured from Polyolefins Industries, Chennai. Characteristics of the used EVA are listed in Table I. Calcium phosphate nanoparticles were prepared and characterized with XRD and TEM as described in Refs. 24–26.

Methods

Preparation of nanocomposites

EVA-calcium phosphate nanocomposites were prepared in an internal mixer at a rotor speed of 60 rpm. The temperature of mixing was 130°C, and the total time for mixing was 10 min. The filler weight percentages were varied as 0.5, 1, 3, 5, and 7. The lumps obtained were compression molded at 130°C to obtain sheets of 2-mm thickness. The samples were designated as E0, E0.5, E1, E3, E5, and E7, respectively.

Transmission electron microscopy

The dispersion of nanocalcium phosphate in EVA matrix has been investigated by TEM. Transmission electron micrographs of the nanocomposites were taken in a Leo 912 Omega transmission electron microscope with an acceleration voltage of 120 keV. The specimens were prepared using an ultracut E cryomicrotone. Thin sections of about 100 nm were cut with a glass knife at room temperature.

Tensile properties of the nanocomposites

Tensile tests were carried out according to ASTM D 412-98a using dumb-bell specimens at 27°C ± 2°C. Samples were punched from compression-molded sheets of thickness 2 mm using a dumb-bell die (C-type). The thickness of the narrow portion was measured using a digital thickness guage. The sample was held tight by two grips in a tensile testing machine (TNE series 5T) the lower of which being fixed. The testing speed was 500 mm/min. The tensile strength

and elongation at break values of the specimen were determined from the stress–strain curves.

Gas permeability testing

The gas permeability of the nanocomposites was measured using Lyssy Manometric Gas Permeability Tester L100-2402. The test gases used were oxygen and nitrogen at a rate of 500 mL/m^2/day. The measurements were performed at 23°C and at a relative humidity of 60 up to equilibrium results. Permeability of the samples was calculated using the equation,

$$P_m = (T_r \times P_r)/t_m \quad (1)$$

where P_m is the permeability of the test sample, t_m is the interval time constant for the test sample, P_r is the permeability of the reference (standard PET sample), and T_r is the interval time constant for standard PET.

Diffusion experiments

The diffusion experiments were carried out with three samples—E0, E3, and E5 only. These samples showed good properties in all other measurements such as mechanical properties, dynamic mechanical properties, and gas permeability tests. Circular samples of 2-cm diameter were cut from polymer sheets by means of a standard die. The thickness and initial weight of the samples were measured. The thickness of the samples was $\sim$ 2 mm. The samples were kept in diffusion bottles at room temperature. The samples were removed from the diffusion bottles periodically and weighed immediately to the nearest $\pm$0.1 mg using electronic balance to reduce the experimental error due to evaporation of solvent. Before each weighing, the surface of the samples was cleaned gently to remove the adhering solvents with minimum pressure using filter paper. Immediately after weighing, the sample is kept back in the diffusion. The experimental procedure was continued until the equilibrium swelling was attained. The results of solvent uptake by the polymer are expressed as mol % of the solvent sorbed by 0.1 kg of the polymer (Q_t). The experiments were duplicates or triplicates in most cases, and the standard deviation was found to range from 0.007 to 0.1 in different cases of solvents. The solvent uptake [Q_t (%)] of the samples was computed using the equation,

$$Q_t\ (\%) = \frac{m_t - m_0}{m_0} \times 100 \quad (2)$$

where m_0 and m_t are the weights of samples before and after a time t of immersion. The experiments were carried out using water, benzene, and *n*-heptane.

RESULTS AND DISCUSSION

Transmission electron microscopy studies

Transmission electron microscopic images of the nanocomposites are given in Figure 1(a–e). The neat EVA gives a clear picture in the TEM image. From the TEM images of the nanocomposites, we can see that the nanoparticles are well dispersed in the matrix. As we go from the low-filler loading, say 0.5%, we can see discrete particles in the matrix. However, the increase in concentration of fillers enables more particle–particle interaction, which promotes the formation of filler agglomerates. Although we go through the images up to 7% filled composites, the particle agglomerates can be clearly seen. When there is good interaction between the polymer matrix and filler, the chances for agglomeration will be less. But owing to the large surface energy for the nanoparticles, when we increase the amount of fillers the particle–particle interaction will increase resulting in agglomerates.

Tensile properties of the nanocomposites

In most of the EVA nanocomposites studied so far, the mechanical properties such as tensile strength, elongation at break, and tensile modulus are reported with respect to the concentration of the fillers.[31–35] Stress–strain behavior of the EVA/calcium phosphate nanocomposites is given in Figure 2. All the composites show similar pattern for the stress–strain curves. We can clearly see two distinct regions, viz., the elastic portion and the orientation of the PE chains. In the initial elastic region, the stress increases regularly and reaches a maximum point and yielding starts. Later due to the orientation of the polyethylene chains, stress values show further increases. Finally, the samples break. In our case, also typical stress–strain curves were obtained for the EVA nanocomposites. From these curves, various parameters such as tensile strength, tensile modulus, and elongation at break were calculated.

The tensile strength and tensile modulus values of the nanocomposites are plotted against the filler content in Figure 3. It can be seen that the tensile strength increases upon addition of nanofillers. On addition of 0.5 wt % of nanofiller, the tensile strength increased by 50% when compared with the neat polymer. But on further increasing the weight percentage of nanofiller, the values decreased. This behavior is explained in terms of two aspects. At low-filler concentrations, the filler and polymer matrix show good interaction. The strong interfacial interaction between the filler and the matrix forms some shear zones when the composites are under stress and strain. Because of this strong interaction and development of shear zones, tensile strength of

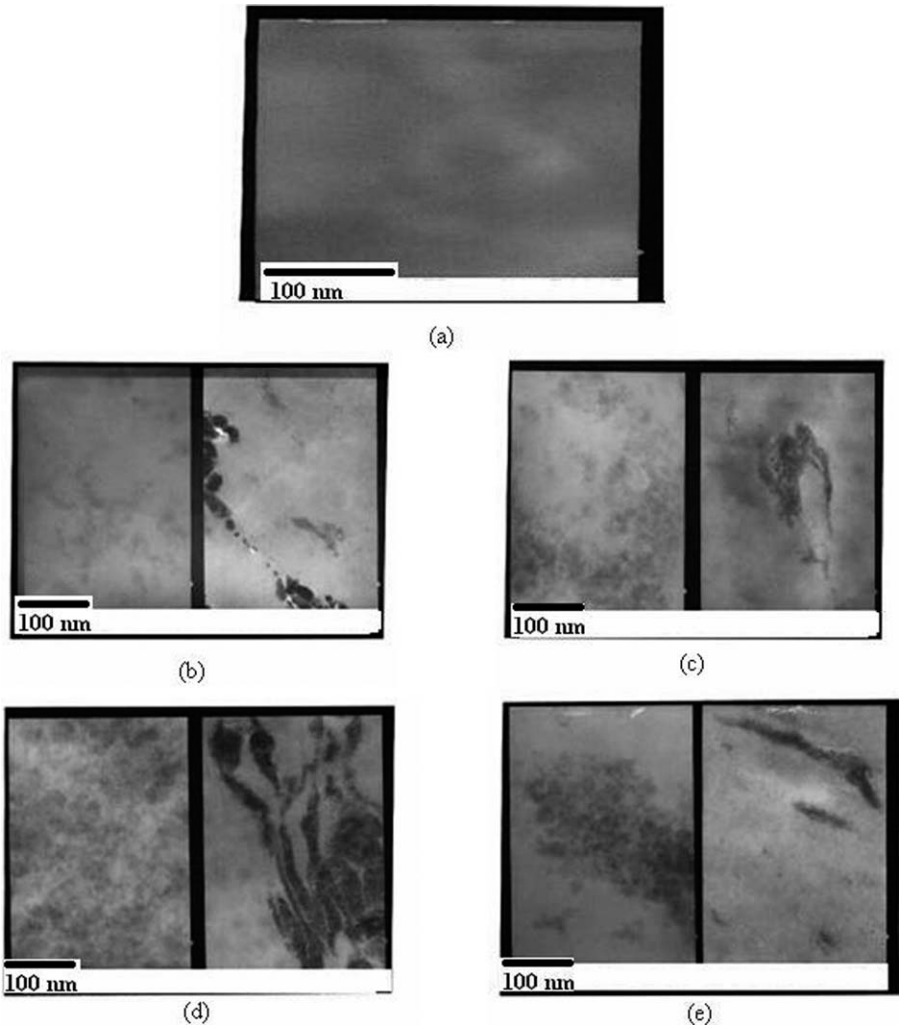

Figure 1 TEM images of EVA-calcium phosphate nanocomposites (a) neat EVA and (b) 1%, (c) 3%, (d) 5%, and (e) 7% filled systems.

the nanocomposites is increased. But, for the increased filler loading, both these parameters show a decreasing trend due to filler–filler interaction.

The nanofilled composites generally show an increase in modulus values. The increase in modulus can be explained due to the good interaction between the filler and the matrix. The nanofillers have high-surface area compared to the conventional fillers and therefore good interaction with the polymer chains. The tensile modulus values of the nanocomposites are also seen from Figure 3. The modulus values increase upon filler addition up to 5% filler loading. For higher loadings, the modulus decreases. This is explained mainly because of the agglomeration of the particles.

Gas permeability studies

The permeation of gases through an organic membrane such as a polymer film is a complex process and has two main stages: initially, the gas molecules are adsorbed on the surface of the membrane, and then they diffuse through the membrane. During adsorption, the gas molecules are occupied in the free volume holes of the polymer that are created by thermal perturbations or by Brownian motions of the chains. The diffusion process occurs by jumps through neighboring holes. Thus, it depends on the number and the size of these holes (static free volume) and on the frequency of the jumps (dynamic free volume). The static free volume is independent of thermal motions of the macromolecules and is related to the gas solubility, whereas the dynamic free volume originates from the segmental motions of the polymer chains and is related to the gas diffusivity. Thus, the diffusion coefficient is a kinetic factor that reflects the mobility of the gas molecules in the polymeric phase, whereas the solubility coefficient is a thermodynamic factor related to the interactions between the polymer and the gas molecules. The nanocomposite is supposed to be consisting of a permeable polymer phase in which impermeable

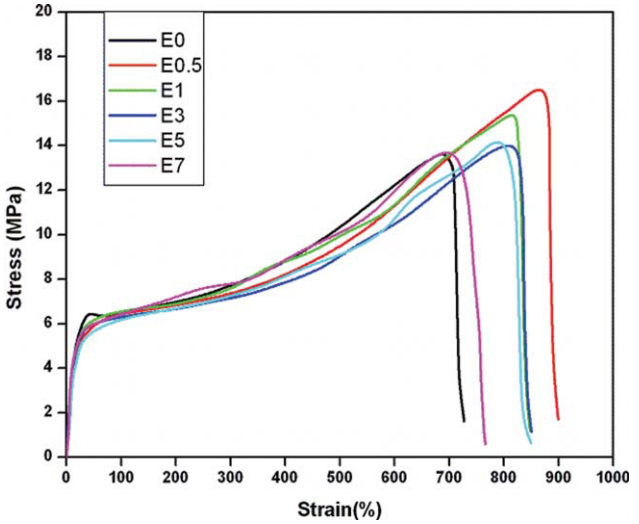

Figure 2 Stress–strain curves of EVA-calcium phosphate nanocomposites. [Color figure can be viewed in the online issue, which is available at wileyonlinelibrary.com.]

nanoparticles are dispersed. There are three main factors that influence the permeability of a nanocomposite: the volume fraction of the nanoparticles, their orientation relative to the diffusion direction, and their aspect ratio. The major factor is the tortuosity, which is connected directly to the shape and the degree of dispersion of the nanoparticles.[36]

Oxygen and nitrogen permeability of the neat polymer and nanocomposites were measured, and the values are given in Table II. From the values, we can clearly seen that the permeability values decreased substantially up on nanofiller addition. Usually, nanofillers have more number of particles compared to micro and macrofillers. This will create more occupation of the voids in the polymer matrix. Hence the gas passing through the composites has to go through a more constrained path due to the occupation of voids by the fillers. Thus, the permeability of the gases will

TABLE II
Permeability Values of the Nanocomposites

Composition	Oxygen permeability (mL/m^2 day)	Nitrogen permeability (mL/m^2 day)
E0	336.96	263.87
E0.5	298.63	251.21
E1	271.69	247.98
E3	264.51	239.65
E5	242.68	221.32
E7	237.53	219.78

decrease. In our case, the composites showed a decrease of about 30 and 20% in oxygen and nitrogen permeabilities, respectively, especially for the 5 wt %-filled systems. The composites with low-filler loading showed maximum decrease in permeability, and, for the composites such as 5 and 7 wt %, the values are almost constant. The penetrability rate of nitrogen gas was found to be smaller than that of oxygen for samples with the same nanofiller content. This is due to the difference in the kinetic diameter of the gases. The kinetic diameter of nitrogen and oxygen is found to be 3.64 Å and 3.46 Å, respectively. Therefore, oxygen will penetrate more compared to nitrogen.

The trend of the data followed models that describe molecular transport through a polymer matrix containing impermeable spherical filler particles, that is, Maxwell's equation

$$P_c = P_p\left(\frac{1-\phi_f}{1+\frac{\phi_f}{2}}\right) \tag{3}$$

where P_c is the permeability of the composite, P_p is the permeability of the pure polymer network, and φ_f is the volume fraction of the filler.[37–39]

Figure 4 shows the variation of permeabilities of oxygen and nitrogen with respect of the volume

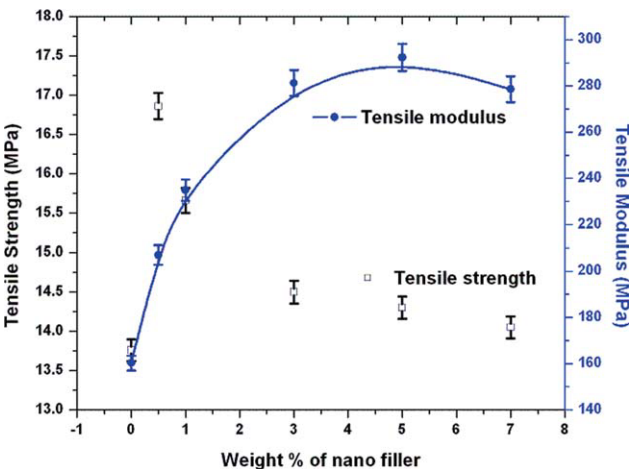

Figure 3 Tensile strength and tensile modulus of EVA nanocomposites. [Color figure can be viewed in the online issue, which is available at wileyonlinelibrary.com.]

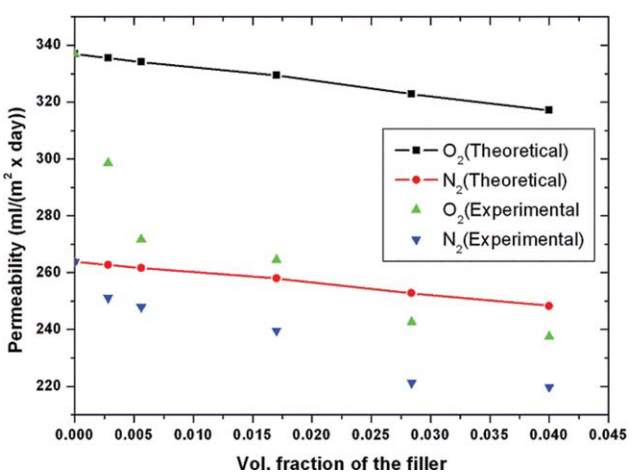

Figure 4 Theoretical model and experimental results of gas permeability of the composites. [Color figure can be viewed in the online issue, which is available at wileyonlinelibrary.com.]

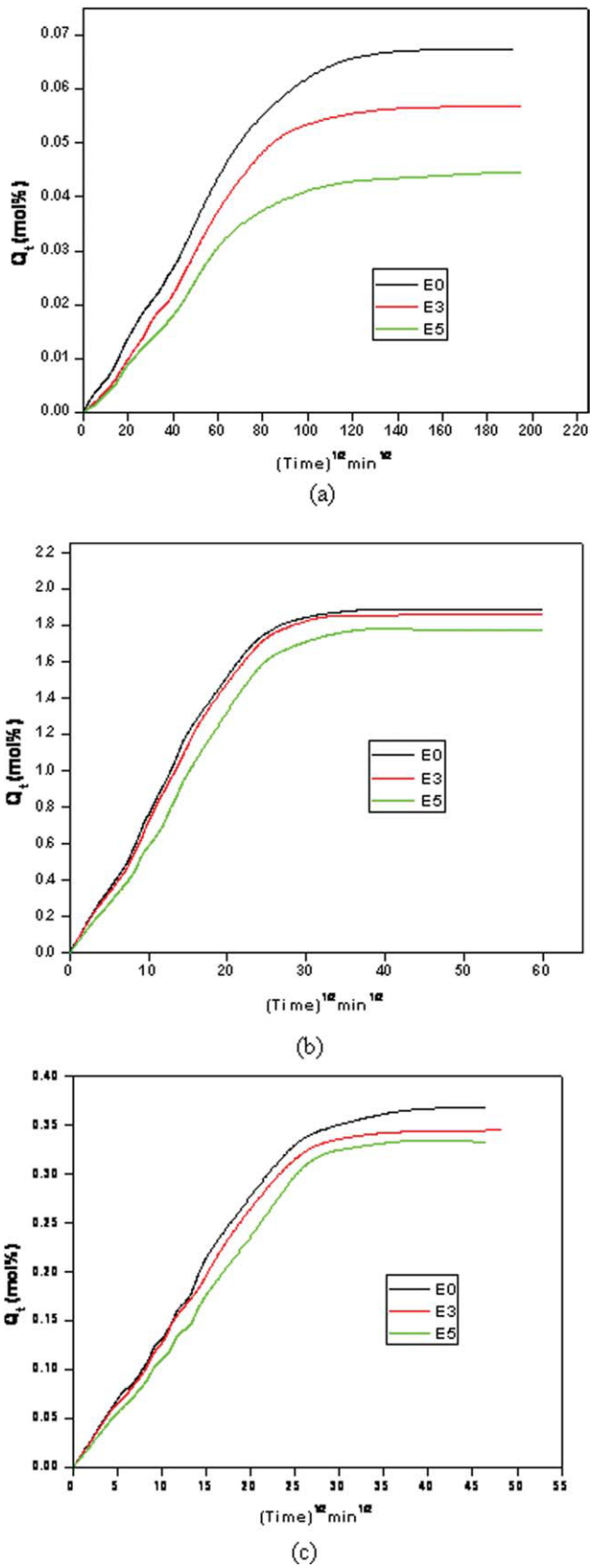

Figure 5 Mol % uptake of solvents through EVA nanocomposites at 27°C (a) water, (b) benzene, and (c) *n*-heptane. [Color figure can be viewed in the online issue, which is available at wileyonlinelibrary.com.]

fraction of the filler content and the behavior with respect to the Maxwell model. We can conclude that the composites show the same trend as depicted by the model. However, the experimental results show more deviation from the theoretical model. This may be due to the better matrix–filler interaction, which created less voids in the system. This aspect has not been included in the model.

Swelling behavior

From the TEM images from Figure 1(a–e), we can see that as we increase the filler concentration the particles tend to form agglomerates. Therefore, the composites with less filler content were selected for molecular transport studies. In addition to this, mechanical and gas permeability studies supplemented that the composites with 3 and 5 wt % showed good properties. Thus, we selected the composites with low-filler loading for the diffusion characteristics. The variation in solvent uptake with increase in filler loading is analyzed using three different solvents viz, water, benzene, and *n*-heptane as the solvents. Figure 5(a–c) shows the change in solvent uptake with time for the nanocomposites. It is found that the absorption of solvent reduced for nanofilled samples than pristine polymer. As we increase filler concentration, the tortuousity of the path increases and hence the solvent uptake decreases. Also, we can see two distinguished zones in the curves. The first zone corresponds to the initial solvent uptake. The swelling rate is too high in this area because of the large concentration gradient, and the polymer sample is under severe solvent stress. The second zone indicates a reduced swelling rate due to the decrease in concentration gradient, which finally reaches at equilibrium swelling. This means that the concentration gradient

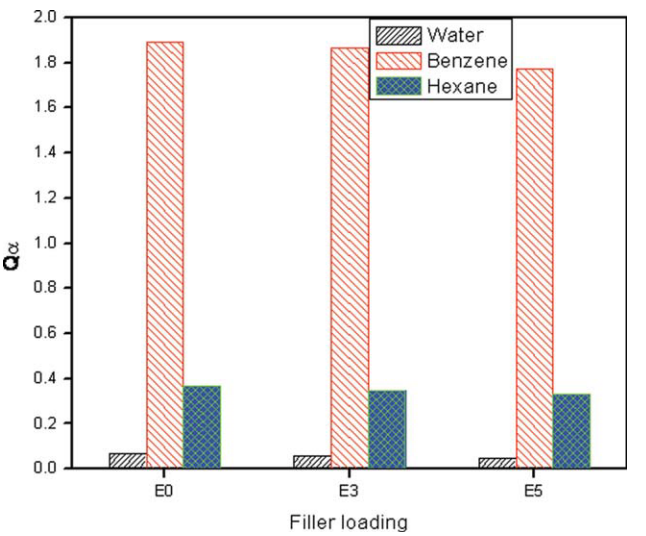

Figure 6 Equilibrium sorption, Q_∞ (mol %) against filler loading. [Color figure can be viewed in the online issue, which is available at wileyonlinelibrary.com.]

TABLE III
Analysis of Sorption Data of EVA Nanocomposites at Room Temperature

	N			$K \times 10^{-2}$		
	E0	E3	E5	E0	E3	E5
Water	0.5	0.57	0.59	0.99	0.53	0.52
Benzene	0.52	0.52	0.56	3.53	3.39	2.58
Heptane	0.50	0.51	0.52	3.6	3.36	3.05

attaining zero value. On increasing the filler concentration after a certain levels, the chances for agglomeration are high, which will lead to more solvent uptake as reported by Stephen et al.[14] These systems also showed filler agglomeration in higher loaded systems.

Solvent uptake in these systems was also studied with aromatic (benzene) and aliphatic (*n*-heptane) liquids. The sorption curves are given in Figure 5(b,c). Both the liquids show more or less similar behavior in the solvent uptake. The pristine polymer showed higher uptake among the three and on increasing the filler loading the uptake decreases due to the increment in tortousity.

Figure 6 represents the equilibrium uptake (Q_∞) against each of the polymer samples. Here, we can see that the aromatic liquid gets absorbed to the polymer much more than that of aliphatic and polar liquids. This is due to the similarity in the structure, that is, both have hydrocarbon constituents in their respective structures. The absorption of water is very less compared to other two liquids.

Mechanism of transport

To investigate the type of transport mechanism, the sorption results were fitted into the following equation[40,41]

$$\log \frac{Q_t}{Q_\alpha} = \log\ k + n\ \log\ t \tag{4}$$

where Q_t and Q_∞ are the mol % solvent uptake at time t and at equilibrium, respectively, and k is a parameter, which depends on the structural characteristics of the polymer in addition to its interaction with the solvent. The value of n indicates the type of the mechanism. The value of $n = 0.5$ indicates Fickian transport, while $n = 1$ shows case II (relaxation controlled) transport. The values of n between 0.5 and 1 indicate an anomalous mode of transport. Also, there have been reports of $n > 1$, which is called super case II.[42]

The values of n and k for all samples in the three solvents at room temperature were determined by regression analysis of the linear portion of plots log (Q_t/Q_∞) versus log t. To assure linearity, the values up to 50% of the equilibrium uptake were only used. The estimated values of n and k are compiled in Table III. For water and *n*-heptane, the n value is 0.5 indicating a Fickian mode of transport. But for benzene there is slight deviation from the Fickian behavior. Although incorporating the nanoparticles, the transport mechanism for water changes from Fickian to non-Fickian as the n values show significant change from 0.5. But for benzene and heptane, the n values are almost same. For all the three systems, the k values are higher for the neat samples. On increasing the filler concentration, the k values decreased owing to the decrease in solvent uptake in each case.

Transport coefficients

From the slope h of the initial linear portion of the sorption curves (Q_t vs. $t_{1/2}$), the diffusion coefficient, D, was calculated using the equation[40,42]

$$D = \pi(h\theta/4Q_\infty)^2 \tag{5}$$

where h is the thickness of the polymer sample and Q_∞ is the equilibrium mol % uptake. Because significant swelling of polymer samples was observed during sorption experiments in all solvents, correction to diffusion coefficients under swollen conditions was essential. This was done by calculating the intrinsic diffusion coefficient D^*, from the volume fraction of polymer in the swollen sample using the relation.[43]

$$D^* = \frac{D}{\phi^{7/3}} \tag{6}$$

The modified diffusion coefficient values known as intrinsic diffusion coefficient are given in the Table IV. We can see that, for all the three solvents,

TABLE IV
Values of D^*, S, and P for EVA Nanocomposites at Room Temperature

	$D^* \times 10^{10}$ ($m^2\ s^{-1}$)			S (gg^{-1})			$P \times 10^{10}$ ($m^2\ s^{-1}$)		
	E0	E3	E5	E0	E3	E5	E0	E3	E5
Water	0.843	0.809	0.774	0.085	0.071	0.048	0.071	0.057	0.037
Benzene	120.9	116.14	93.42	2.41	2.30	1.91	291.19	267.88	178.67
Heptane	16.93	15.40	13.90	0.468	0.425	0.382	7.92	6.54	5.311

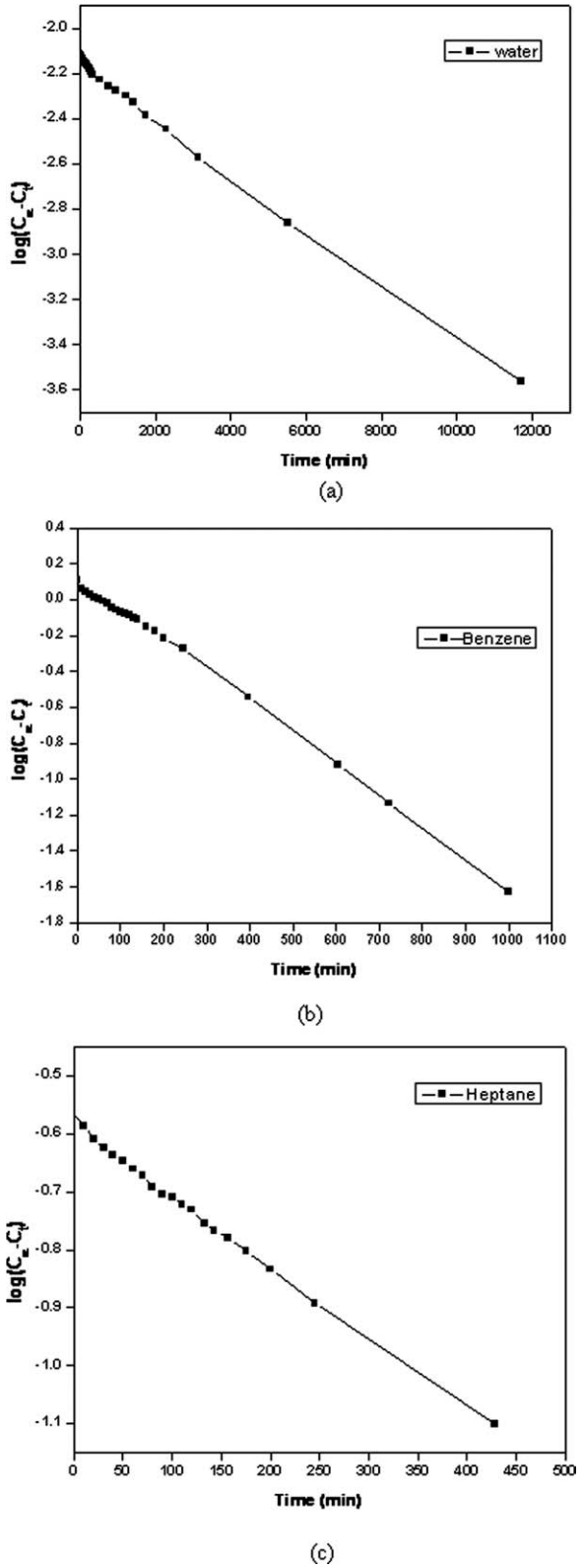

Figure 7 First-order kinetics plot of E3 samples in (a) water, (b) benzene, and (c) *n*-heptane.

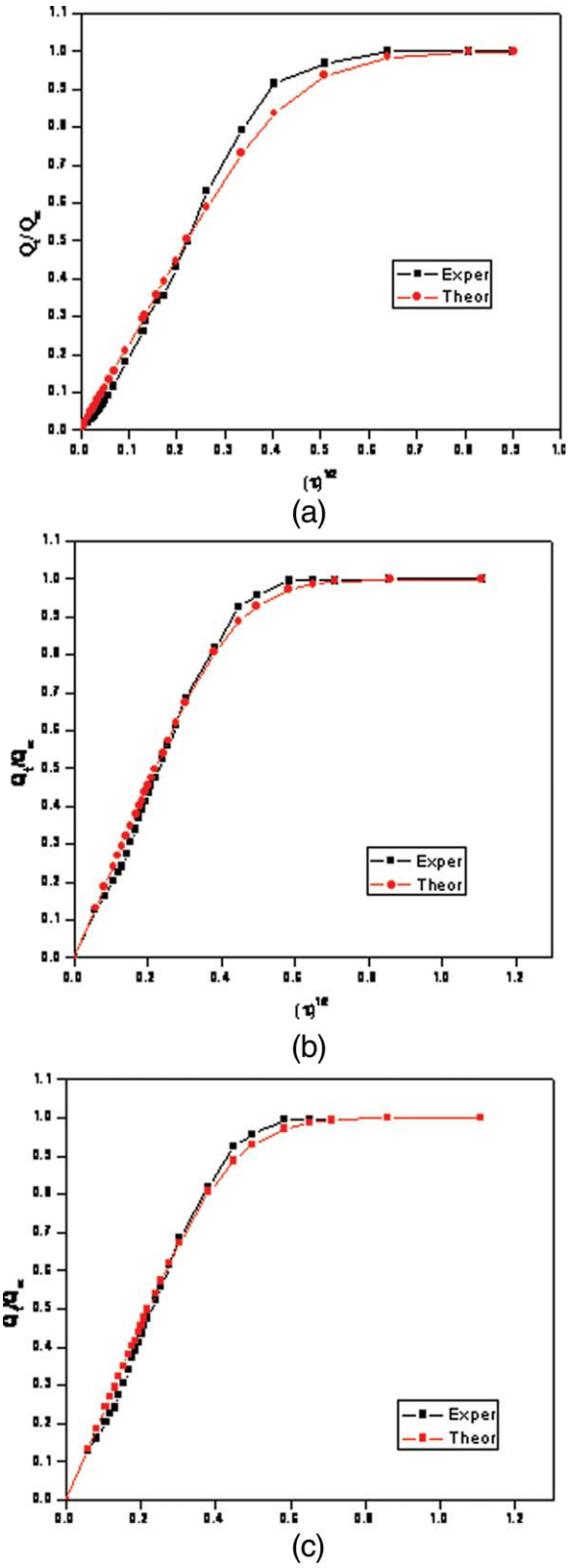

Figure 8 Theoretical and experimental sorption curves of E3 samples in (a) water, (b) benzene, and (c) *n*-heptane. [Color figure can be viewed in the online issue, which is available at wileyonlinelibrary.com.]

the D^* values decrease from E0 to E5 regularly. Thus, when the concentration of particles increases, the intrinsic diffusion coefficient values decrease.

The permeation of a penetrant into a polymer membrane depends on the diffusivity as well as on the sorption. Hence sorption coefficient is calculated using the equation[44]

$$S = \frac{M_\infty}{M_0} \tag{7}$$

where M_∞ is the mass of the solvent at equilibrium swelling and M_0 is the initial polymer mass. S values are given in Table IV for all the composites and for three different solvents. We can see that the sorption coefficient decreased with respect to the filler loading for all the three solvents. This is expected from the sorption curves previously. Here, also, benzene has the higher values and water has very low values.

Permeation is a collective process of diffusion and sorption, and hence permeation coefficient, P, can be defined as[41,42]

$$P = D^* \times S \tag{8}$$

where D^* is the intrinsic diffusion coefficient and S, the sorption coefficient. Permeation coefficient, P, is given in Table IV. Note that with respect to the filler loading, the values decrease and aromatic solvent has the higher values among these solvents.

Transport kinetics

The kinetics of transport of solvents through E3 nanocomposites was studied by first-order kinetics.[45] The first-order equation is

$$k_1 t = \ln \frac{C_\infty}{(C_\infty - C_t)} \tag{9}$$

where k_1 is the first-order rate constant, and C_t and C_∞ represent concentration at a time t and at equilibrium. Plot of log $(C_\infty - C_t)$ versus time is shown in Figure 7(a–c). All the three curves showed straight-line graphs. Thus, we can conclude that the transport follows first-order kinetics.

Theoretical modeling

The kinetics of solvent uptake of the dense polymeric materials is often fitted according to the following equations[46]:

$$Q_t/Q_\alpha = 4(\tau/\pi)^{1/2} \text{ for } \tau \leq 0.049 \tag{10}$$

$$\text{w/w (eq)} = \left(1 - \frac{8}{\pi^2}\right) \sum_0^\infty \frac{1}{(2n+1)^2} \exp[-(2n+1)^2 \pi^2 \tau] \quad \text{for } \tau > 0.049 \tag{11}$$

where τ is a dimensionless parameter ($\tau = D_t/h^2$). The theoretical curves for the sorption of solvents through E3 nanocomposites are given in Figure 8(a–c). Here, we can see that the theoretical curves almost match with the experimental curves. For benzene and heptane, the theoretical curves very slight deviation in the initial and leveling off region. But in the case of water, the experimental curve shows some deviation in the leveling-off region. We noted that the n value obtained E3 for water sorption is 0.57, while for benzene and heptane, it was 0.52 and 0.51, respectively. So, this deviation reflected in the theoretical curves too.

CONCLUSIONS

PEVA/calcium phosphate nanocomposites were prepared by the melt-mixing technique. The nanoparticles were prepared by the polymer-induced crystallization technique. The mechanical properties of the composites showed marked improvement with low-filler loading. The oxygen and nitrogen gas permeability of the composites showed good reduction, which will be beneficial for suitable applications of these materials. Molecular transports of different solvents were analyzed at room temperature with respect to the filler loading. The composites showed marked decrease in uptake compared to the neat polymer. This is attributed to the more tortuous path created by the nanofillers in the composites.

References

1. Giannellis, E. P. Adv Mater 1996, 8, 29.
2. Wu, Y.-P.; Zhang, L.-Q.; Wang, Y.-Q.; Liang, Y.; Yu, D.-S. J Appl Polym Sci 2001, 82, 2842.
3. Krishnamoorti, R.; Vaia, R. A.; Giannelis, E. P. Chem Mater 1996, 9, 1728.
4. Zanetti, M.; Lomakin, S.; Camino, G. Macromol Mater Eng 2000, 279, 1.
5. George, S. C.; Thomas, S. Prog Polym Sci 2001, 26, 985.
6. Mathew, A. P.; Packirisamy, S.; Stephen, R.; Thomas, S. J Membr Sci 2002, 201, 213.
7. George, S. C.; Groeninckx, G.; Ninan, K. N.; Thomas, S. J Polym Sci Part B: Polym Phys 2000, 38, 2136.
8. George, S. C.; Thomas, S.; Ninan, K. N. Polymer 1996, 37, 5839.
9. Unnikrishnan, G.; Thomas, S. Polymer 1998, 39, 3933.
10. Joseph, A.; Mathai, A. E.; Thomas, S. J Membr Sci 2003, 220, 13.
11. Prasanthakumar, R.; Thomas, S. J Adhes Sci Technol 2001, 15, 633.
12. Varghese, S.; Kuriakose, B.; Thomas, S.; Joseph, K. Rubber Chem Technol 1995, 68, 37.
13. Pomerantsev, A. L. J Appl Polym Sci 2005, 96, 1102.
14. Stephen, R.; Varghese, S.; Joseph, K.; Oommen, Z.; Thomas, S. J Membr Sci 2006, 282, 162.
15. Stephen, R.; Joseph, K.; Oommen, Z.; Thomas, S. Compos Sci Technol 2007, 67, 1187.
16. Beyer, G. Fire Mater 2001, 25, 193.
17. Anil Kumar, S.; Yuelong, H.; Yumei, D.; Le, Y.; Kumaran, M. G.; Thomas, S. Ind Eng Chem Res 2008, 47, 4898.
18. Shi, Y.; Kashiwagi, T.; Walters, R. N.; Gilman, J. W.; Lyon, R. E.; Sogah, D. Y. Polymer 2009, 50, 3478.

19. George, J. J.; Bhowmick, A. K. Nanoscale Res Lett 2008, 3, 508.
20. Lee, H. M.; Park, B. J.; Choi, H. J.; Gupta, R. K.; Bhattacharya, S. N. J Macromol Sci Part B: Phys 2007, 46, 261.
21. Radhakrishnan, S. J Cryst Growth 1994, 141, 437.
22. Saujanya, C.; Radhakrishnan, S. J Mater Sci 1998, 33, 1063.
23. Saujanya, C.; Radhakrishnan, S. Polymer 2001, 42, 6723.
24. Thomas, S. P.; Thomas, S.; Abraham, R.; Bandyopadhyay, S. eXPRESS Polym Lett 2008, 2, 528.
25. Thomas, S. P.; Thomas, S.; Bandyopadhyay, S.; Wurm, A.; Schick, C. Compos Sci Technol 2008, 68, 3220.
26. Thomas, S. P.; Thomas, S.; Bandyopadhyay, S. J Phys Chem C 2009, 113, 97.
27. Patil, C. B.; Shisode, P. S.; Kapadi, U. R.; Hundiwale, D. G.; Mahulikar, P. P. Mater Sci Eng B 2010, 168, 231.
28. Dorozhkin, S. V. Acta Biomater 2010, 6, 715.
29. Xu, H. H. K.; Weir, M. D.; Sun, L. Dent Mater 2007, 23, 1482.
30. Hiemstra, T.; Antelo, J.; (Debby) van Rotterdam, A. M. D.; van Riemsdijk, W. H. Geochim Cosmochim Acta 2010, 74, 59.
31. Alexandre, M.; Beyer, G.; Henrist, C.; Cloots, R.; Rulmont, A.; Jerome, R.; Dubois, P. Macromol Rapid Commun 2001, 22, 643.
32. Alexandre, M.; Beyer, G.; Henrist, C.; Cloots, R.; Rulmont, A.; Jerome R.; Dubois, P. Chem Mater 2001, 13, 3830.
33. Pramanik, M.; Srivastava, S. K.; Samantaray, B. K.; Bhowmick, A. K. J Mater Sci Lett 2001, 20, 1377.
34. Tang, Y.; Hu, Y.; Wang, J.; Zong, R.; Gui, Z.; Chen, Z.; Zhuang, Y.; Fan, W. J Appl Polym Sci 2004, 91, 2416.
35. Srivastava, S. K.; Pramanik, M.; Acharya, H. J Polym Sci Part B: Polym Phys 2006, 44, 471.
36. Freeman, B. D. Macromolecules 1999, 32, 375.
37. Barrer, R. M. In Diffusion in Polymers; Crank, J.; Park, G. S., Eds.; Academic Press: New York, 1968; p 165.
38. Maxwell, C. Treatise on Electricity and Magnetism; Oxford University Press: London, 1873.
39. Comer, A. C.; Kalika, D. S.; Kusuma, V. A.; Freeman, B. D. J Appl Polym Sci 2010, 117, 2395.
40. Aminabhavi, T. M.; Phayde, H. T. S. Polymer 1995, 36, 1023.
41. Chiou, J. S.; Paul, D. R. Polym Eng Sci 1986, 26, 1218.
42. Vieth, W. R. Diffusion In and Through Polymers: Principles and Applications; Oxford University Press: New York, 1991.
43. Kumar, P. V. A.; Varughese, K. T.; Thomas, S. Polym Polym Compos 2002, 10, 553.
44. Mathew, A. P.; Packirisamy, S.; Kumaran, M. G.; Thomas, S. Polymer 1995, 36, 4935.
45. Aminabhavi, T. M.; Harogoppad, S. B. J Chem Educ 1991, 68, 343.
46. Crank, J. The Mathematics of Diffusion. Clarendon Press: Oxford, 1957.